ELLIPTIC FLOW MEASURED IN THE CERES/NA45 EXPERIMENT

S. I. Esumi, J. Slívová and J. Milošević for the NA45/CERES Collaboration

D. Adamová [a], G. Agakichiev [b], H. Appelshäuser [c], V. Belaga [d], P. Braun-Munzinger [b], A. Cherlin [e], S. Damjanović [c], T. Dietel [c], L. Dietrich [c], A. Drees [f], S. I. Esumi [c], K. Filimonov [c], K. Fomenko [d], Z. Fraenkel [e], C. Garabatos [b], P. Glässel [c], G. Hering [b], J. Holeczek [b], V. Kushpil [a], B. Lenkeit [g], W. Ludolphs [c], A. Maas [b], A. Marín [b], F. Messer [c], M. Messer [c], J. Milošević [c], A. Milov [e], D. Miśkowiec [b], Y. Panebrattsev [d], O. Petchenova [d], V. Petráček [c], A. Pfeiffer [g], N. Raičević [d], J. Rak [b], I. Ravinovich [e], P. Rehak [h], M. Richter [c], H. Sako [b], H. Schäfer [c], W. Schmitz [c], J. Schukraft [g], S. Sedykh [b], W. Seipp [c], S. Shimansky [d], J. Slívová [c], H. J. Specht [c], J. Stachel [c], M. Šumbera [a], H. Tilsner [c], I. Tserruya [e], J. P. Wessels [c], C. Voigt [c], T. Wienold [c], B. Windelband [c], J. P. Wurm [i], W. Xie [e], S. Yurevich [c], V. Yurevich [d]

[a] NPI/ASCR, Řež, Czech Republic
[b] GSI, Darmstadt, Germany
[c] Physikalisches Institut, Universität Heidelberg, Germany
[d] JINR, Dubna, Russia
[e] Weizmann Institute, Rehovot, Israel
[f] Department for Physics and Astronomy, SUNY Stony Brook, USA
[g] CERN, Geneva, Switzerland
[h] Brookhaven National Laboratory, Upton, USA
[i] Max-Planck-Institut für Kernphysik, Heidelberg, Germany

Abstract

The CERES/NA45 experiment at the CERN-SPS investigated Pb+Au collisions at 40, 80 and 158 AGeV/c. Using a Fourier analysis of the azimuthal distributions of charged particles (mostly pions) the magnitude of elliptic flow is studied. For these particles we found a small in-plane elliptic flow. The results smoothly fit into the beam energy dependence of the magnitude of elliptic flow connecting the measurements at AGS and RHIC. The centrality dependence shows a decrease of the elliptic flow going from semicentral to the most central collisions, while we observe an increase of elliptic flow with p_T. Calculations performed with the UrQMD model reproduce the p_T integrated data rather well.

The differential second Fourier coefficient of the azimuthal momentum distribution, known as elliptic flow, is defined as $v_2(\mathcal{D}) = \langle\cos(2\phi)\rangle_{\mathcal{D}}$ [1, 2, 3, 4]. The brackets denote averaging over many events, and $\mathcal{D}$ represents a phase-space window in the (p_T, y) plane in which the v_2 value is calculated. The azimuthal angle ϕ is measured with respect to the reaction plane which is defined by the impact parameter vector $\mathbf{b}$ and the beam direction. Over a broad range of beam energies, elliptic flow can be attributed to a competition between the expansion of produced hadrons and the passage time which determines the shadowing effect on these hadrons by the projectile and target spectators [5, 6, 7]. If the passage time is long compared to the expansion time, spectator nucleons block the path of produced hadrons into the reaction plane, and hadrons are squeezed-out perpendicular to this plane resulting in a negative elliptic flow. For shorter passage times, the blocking of hadrons is reduced and preferential in-plane emission or positive elliptic flow appears. For non-central collisions ($b \neq 0$), v_2 is an important observable due to its sensitivity to rescattering of hadrons created in the hot and dense nuclear matter. Thus, it is one of the probes of the hot stages of the collision and may provide information on the equation of state, and especially on a possible phase transition to a new state of matter, the Quark Gluon Plasma.

The CERES/NA45 experiment consists of two radial Silicon Drift Detectors (SDD), two Ring Imaging CHerenkov (RICH) detectors and a radial drift Time Projection Chamber (TPC) which replaced the previously used MultiWire Proportional Chamber (MWPC). Most of the detected particles are charged pions. The SDDs located behind the target have full azimuthal acceptance (ϕ_{lab}) and cover the central rapidity region which is very interesting for elliptic flow measurement. They also provide the possibility to determine the centrality of the collision via the measurements of the charged particle multiplicity. We used the SDDs to study the pseudorapidity (η) and centrality dependence of elliptic flow. The p_T dependence of v_2 was studied in the range ($0.1 < p_T < 2.0$ GeV/c) using the TPC, which is operated inside a magnetic field, providing a precise determination of the momentum. The main purpose of the RICH detectors, placed behind the SDDs, is electron identification. However, they also allow to identify high-p_T pions and measure their momenta ($p_T \geq 1$ GeV/c). The momentum dependence of the elliptic flow of these pions will be presented in this contribution. The more detailed description of the CERES/NA45 experiment can be found in [8, 9, 10, 11].

As data, we used 300k Pb+Au events at 158 AGeV collected in ’96, and 1.5M events at 40 AGeV obtained from the ’99 data taking period.

For the high-p_T pion flow analysis we used the full set (42M) of events recorded in '96. During the 2000 run, CERES was operated with a very good overall performance. For this contribution we made a preliminary analysis on 380k central 80 AGeV Pb+Au events collected in the last year.

For the flow analysis we calculated v_2' with respect to the estimated reaction plane. In order to avoid autocorrelations, short range physics effects or detector correlations, it is useful to determine the reaction planes in different subsamples in slices of ϕ_{lab}. We used four sets of slices in ϕ_{lab} by dividing the full azimuthal acceptance into 100 equal pieces. Each fourth piece belongs to one of the four sets (i=1,2,3 or 4) as it is schematically drawn in Figure 1. For such a choice, each of the sets is still large enough to allow to distinguish a real anisotropy from statistical fluctuations and also to avoid above mentioned effects.

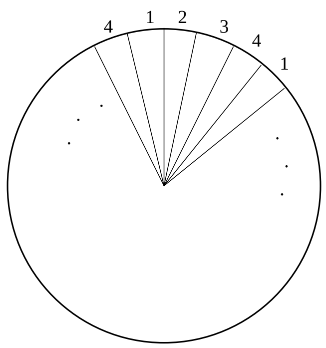

Figure 1: Schematic definition of subsamples in ϕ_{lab}. Each of four sets of slices (i) consists of 25 equal (3.6 deg.) slices. In each of them we performed the same kind of analysis.

The azimuthal angle of the estimated reaction plane in each set of slices is obtained using

$$\Phi_2^{(i)} = \frac{1}{2}\arctan\left(\frac{Y_2^{(i)}}{X_2^{(i)}}\right) \equiv \frac{1}{2}\arctan\left(\frac{\sum \sin(2\phi_{lab}^{(i)})}{\sum \cos(2\phi_{lab}^{(i)})}\right). \quad (1)$$

Biases due to the finite detector acceptance in ϕ_{lab} cause the distributions $(X_2^{(i)}, Y_2^{(i)})$ to shift from the center of the transverse (x, y) plane. We removed this effect by recentering the $(X_2^{(i)}, Y_2^{(i)})$ distributions to their mean values. After recentering, the reaction plane angle distributions were still azimuthally anisotropic in the laboratory system. Assuming a random distribution of the impact parameter vector, it could be removed by making the reaction plane angle distributions isotropic in the laboratory. For that we used the flattening method outlined in [2, 3, 12]. As an example, in Figure 2 (top) is shown the reaction plane angle distribution $dN/d\Phi_2^{(1)}$ (for the 1-st set of slices) before any correction. The huge anisotropy is present. Recentering procedure (middle part of the Figure 2) removed a lot of anisotropy, but still left some small anisotropy. After the flattening (bottom panel on Figure 2) we finally obtained the flat reaction plane angle distribution.

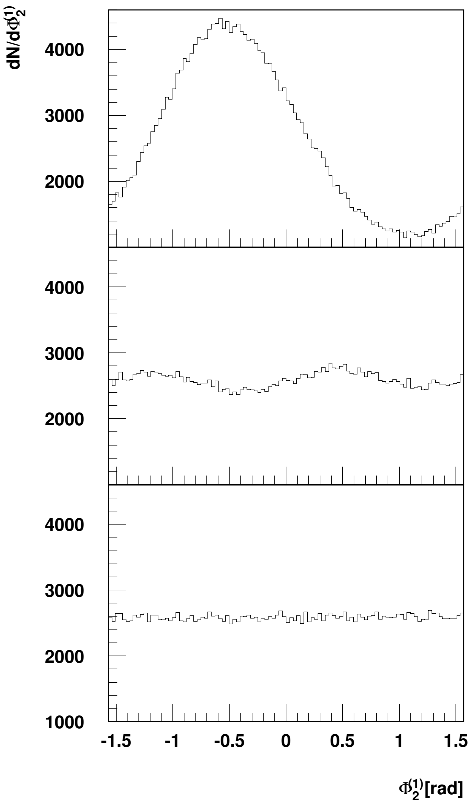

Figure 2: An example of the reaction plane angle distribution before any corrections (top), after recentering (middle), and after the flattening (bottom).

After these corrections, the resolution in the determination of the reaction plane in each set of slices (i) is obtained in the following way. First, we calculated resolutions (Eq. 16 in [3]) for two of three different [1] (j, k) set of slices combinations by

$$\langle\cos[2(\Phi_2^{(i)} - \Phi_2)]\rangle = \sqrt{\frac{\langle\cos[2(\Phi_2^{(i)} - \Phi_2^{(j)})]\rangle\langle\cos[2(\Phi_2^{(i)} - \Phi_2^{(k)})]\rangle}{\langle\cos[2(\Phi_2^{(j)} - \Phi_2^{(k)})]\rangle}}, \qquad (2)$$

where Φ_2 is the true reaction plane azimuthal angle. The indexes i, j and k correspond to the different sets of ϕ-slices ($i \neq j \neq k$) and j and k should satisfy the following relation: $|j - k| = 1$. The resolution which we used for corecting the flow parameters is the average value of the resolutions

[1] We rejected third possible combination in order to maximaly decrease the autocorrelation effect.

obtained from above mentioned two different resolutions. Dividing the observed flow parameters $v_2'^{(i)}$ by the resolution $\langle\cos[2(\Phi_2^{(i+2)} - \Phi_2)]\rangle$ we obtained the corrected flow parameters $v_2^{(i)}$. The final value of v_2 was obtained as a mean value of four $v_2^{(i)}$ values obtained from four sets of slices.

Figure 3 shows the η dependence of the elliptic flow at different centralities for three different energies. The flow was calculated from hits in SDD1 and SDD2. The results, obtained independently from the two silicon detectors, agree very well. Independent of the centrality and the beam energy, the magnitude of elliptic flow shows no significant dependence on the pseudorapidity in the midrapidity region. It is visible that the magnitude of elliptic flow decreases going from semicentral to the most central collisions at all beam energies. Calculations performed with the UrQMD model reproduce the experimental results rather well. A difference between the model and the experiment appears only for semicentral collisions at the lowest energy.

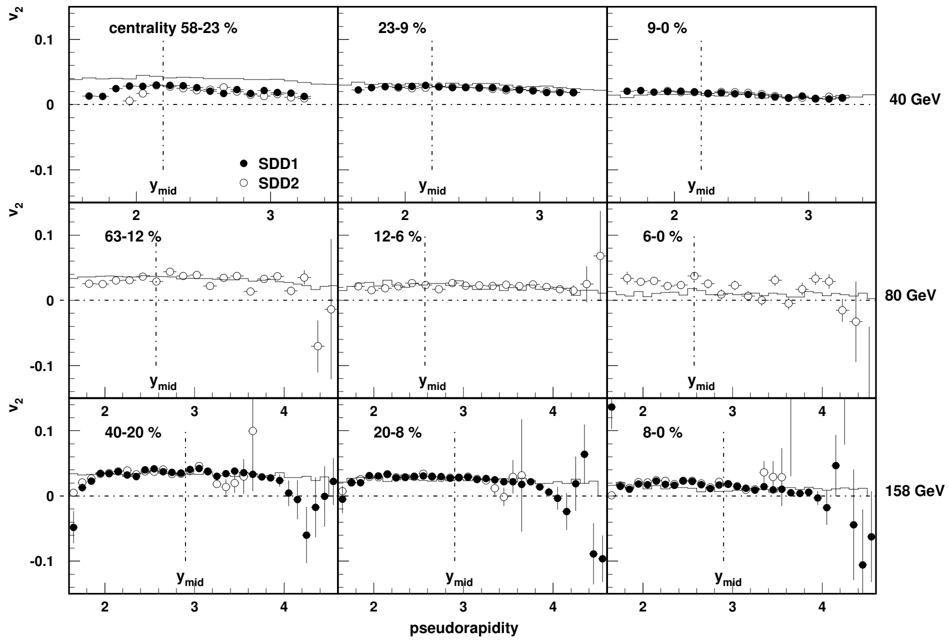

Figure 3: The pseudorapidity dependence of the elliptic flow at different centralities in 40 (top), 80 (middle) and 158 AGeV/c (bottom) Pb+Au collisions.

In Figure 4 (left) is shown the p_T dependence of elliptic flow of identified high-p_T pions identified in the RICH system (triangles), charged particles detected in the MWPC (open circles) and low-p_T pions detected in the NA49 experiment (filled circles) [13] at 158 AGeV/c. Following the low-p_T trend of the NA49 data, both CERES sets of results show an increase of v_2 with increasing p_T. On the right side of Figure 4 is shown a preliminary result of the p_T dependence of elliptic flow for charged particles (95% of them are charged pions) detected in the TPC at a beam energy of 80 AGeV/c. Again, we observed the same trend as mentioned above.

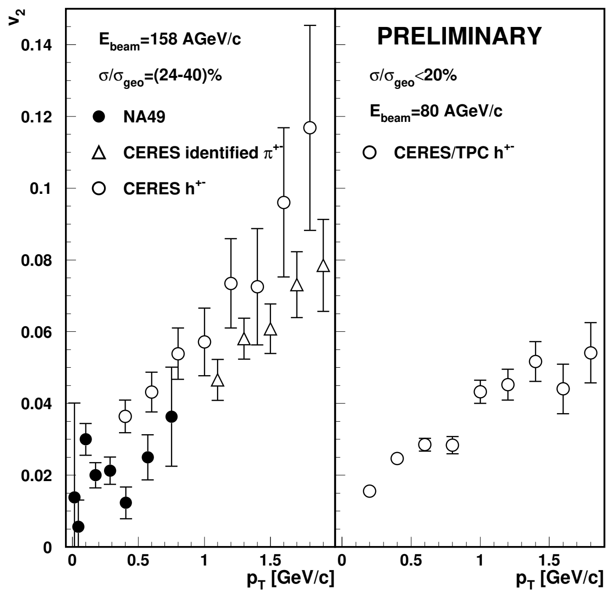

Figure 4: The transverse momentum dependence of the elliptic flow at 158 (left) and 80 AGeV/c (right).

Figure 5 summarizes the results of the elliptic flow measurements at midrapidity in heavy-ion collisions at beam energies from 100 AMeV to 10 ATeV. At beam energies lower than 4A GeV elliptic flow is negative, the elliptic flow is out-of-plane, indicating the dominance of the shadowing. At beam energies higher than 4 AGeV elliptic flow becomes positive, indicating a transition to in-plane elliptic flow and dominance of the initial pressure gradient. The magnitude of in-plane elliptic flow rises slowly with increasing beam energy. This trend is continued also in the recent elliptic flow measurements from STAR at RHIC [14]. From 2% at AGS [12], the p_T averaged in-plane elliptic flow rises to 3% and 4% at SPS [13, 9] and reaches 6% at RHIC [14]. The energy dependence of the elliptic flow might be very important in order to establish the existence of QGP. A nonmonotonic behavior at some specific energy could hint at a significant change in the equation of state of hot and dense nuclear matter, indicating a phase transition.

Using a Fourier analysis of the charged particles azimuthal distri-

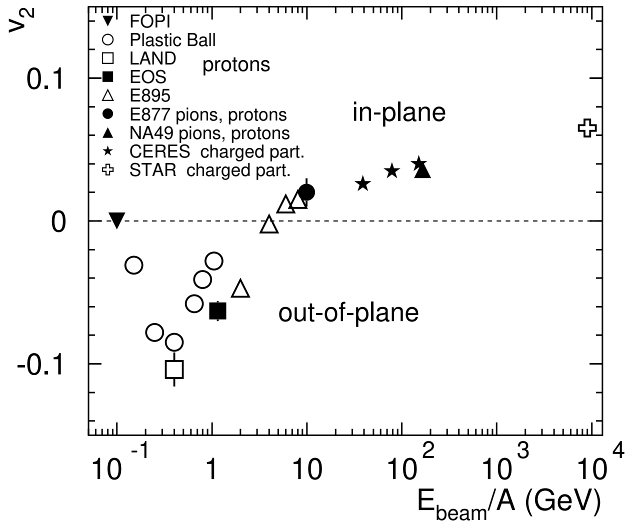

Figure 5: The beam energy dependence of the elliptic flow from SIS/BEVALAC to RHIC energies.

butions we measured the magnitude of elliptic flow in the CERES/NA45 experiment. We found that independent of the centrality and beam energy the elliptic flow does not show a significant dependence on the pseudorapidity. At all beam energies, the magnitude of elliptic flow decreases with centrality and increases with p_T. The UrQMD model results are in a rather good agreement with the experimental ones. The energy dependence of the elliptic flow smoothly connects the magnitude of that flow found at AGS and RHIC energies.

Acknowledgments

The authors wish to thank to the CERN staff. We are gratefull for the financial support by the German BMBF, the U.S. DoE, the MINERVA Foundation and the Israeli Science Foundation.

References

[1] S.Voloshin and Y.Zhang, Z.Phys.C 70 (1996) 665

[2] E877 Collaboration, J.Barrette et al., Phys.Rev.C 55 (1997) 1420

[3] A.M.Poskanzer and S.A.Voloshin, Phys.Rev.C 58 (1998) 1671

[4] N.Borghini, P.M.Dinh and J-Y.Ollitrault, Phys.Rev.C (2001)

[5] H.Sorge, Phys.Rev.Lett. 78 (1997) 2309

[6] P.Danielewicz et al., Phys.Rev.Lett. 81 (1998) 2438

[7] H.Liu, S.Panitkin and N.Xu, Phys.Rev.C 59 (1999) 348

[8] P.Holl et al., Nucl.Inst. and Meth. A377 (1996) 367

[9] H.Appelshäuser for the CERES Collaboration, Nucl.Phys.A 698 (2002) 253c

[10] B.Lenkeit for the CERES Collaboration, Nucl.Phys.A 661 (1999) 23c

[11] A.Marín for the CERES Collaboration, Nucl.Phys.A 661 (1999) 673c

[12] E877 Collaboration, J.Barrette et al., Phys.Rev.C 56 (1997) 3254

[13] NA49 Collaboration, H.Appelshäuser et al., Phys.Rev.Lett. 80 (1998) 4136

[14] STAR Collaboration, K.H.Ackermann et al., Phys.Lett. 86